ORIGINAL ARTICLE

The tyrosyl-DNA phosphodiesterase gene family in *Medicago truncatula* Gaertn.: bioinformatic investigation and expression profiles in response to copper- and PEG-mediated stress

Anca Macovei · Alma Balestrazzi ·
Massimo Confalonieri · Daniela Carbonera

Abstract The *Tdp1* gene encoding tyrosyl-DNA phosphodiesterase has been extensively investigated in animal cells, due to the role of this enzyme in the repair of topoisomerase I-DNA covalent lesions. In contrast, information in this regard is totally missing in plants. We report for the first time in plants on the *Tdp1* gene family from barrel medic (*Medicago truncatula* Gaertn.), composed of two members, hereby named *MtTdp1α* and *MtTdp1β*. The expression profiles of *MtTdp1α* and *MtTdp1β* genes were evaluated in plantlets grown in vitro using copper and polyethylene glycol (PEG 6000) as stress agents. In situ detection of reactive oxygen species (ROS) was carried out by histochemical staining, while the level of oxidative DNA damage, quantified in terms of 7,8-dihydro-8-oxoguanine (8-oxo-dG), increased up to 7.4- and 6.7-fold in response to copper and PEG 6000 treatments, respectively. Quantitative real-time polymerase chain reaction revealed that both *Tdp1* genes were significantly up-regulated in response to copper and PEG. The *Tdp1* genes were also significantly up-regulated during seed rehydration, an aspect of seed physiology in which DNA repair is a key component. Thus, the *Tdp1* genes might be used as novel tools for improving stress tolerance in crops. The expression patterns of the barrel medic *top1α* and *top1β* genes, encoding distinct isoforms of DNA topoisomerase I, were also analyzed and discussed to acquire additional information on their specific functions, closely related to that of the *Tdp1* gene in animal cells.

Abbreviations

Tdp	Tyrosyl-DNA phosphodiesterase
ROS	Reactive oxygen species
8-oxo-dG	7, 8-Dihydro-8-oxoguanine
PEG	Polyethylene glycol
QRT-PCR	Quantitative real-time polymerase chain reaction
top1	Gene encoding DNA topoisomerase I
topo I	DNA topoisomerase I
Mt	*Medicago truncatula*
DAB	3, 3′-Diaminobenzidine
NBT	Nitroblue tetrazolium
APX	Ascorbate peroxidase

Electronic supplementary material The online version of this article (doi:10.1007/s00425-010-1179-9) contains supplementary material, which is available to authorized users.

A. Macovei · A. Balestrazzi · D. Carbonera (✉)
Dipartimento di Genetica e Microbiologia,
Via Ferrata 1, 27100 Pavia, Italy
e-mail: carbo@ipvgen.unipv.it

M. Confalonieri
C.R.A. Centro di Ricerca per le Produzioni Foraggere e
Lattiero-Casearie, Viale Piacenza 29, 26900 Lodi, Italy

Introduction

The enzyme tyrosyl-DNA phosphodiesterase (Tdp1) (EC: 3.1.4), so far investigated only in animal cells, catalyzes the hydrolysis of 3′-phosphotyrosyl bonds formed in vivo between the catalytic tyrosine residue of DNA topoisomerase I (topo I) and the 3′ DNA terminus (Yang et al. 1996). The catalytic mechanism of topo I includes (1) DNA cleavage, (2) relaxation, (3) religation of the same DNA strand and (4) dissociation of the enzyme from DNA (Schoeffler

and Berger 2008). When topo I binds DNA sites with modified nucleotides, e.g., the oxidized base 7,8-dihydro-8-oxoguanine (8-oxoG) or when the enzyme interacts with the anticancer drug camptothecin, the religation step is blocked (Pommier et al. 2003). As a consequence, topo I becomes covalently trapped at the 3′ end of the cleaved DNA strand with deleterious effects on cell viability.

The Tdp1 protein is characterized by two HKD motifs containing the conserved amino acid residues of the active site (Interthal et al. 2001). During the Tdp1 reaction, a histidine residue (namely His-263 in the human enzyme) is responsible for the nucleophilic attack against the phosphorus atom linking the catalytic tyrosine of topo I and the 3′-oxygen of the nucleotide. The Tdp1 enzyme binds itself to DNA, replacing the tyrosine residue. As a result, a Tdp1-DNA covalent complex is formed. Subsequently, another histidine (His-493 in the human protein), located within the C-terminal HKD motif, activates a water molecule with the consequent hydrolysis of the His-263/DNA bond and the release of the enzyme. In the human *Tdp1* gene, a mutation involving His-493 has been recognized as the cause of a heritable neurodegenerative disorder (Takashima et al. 2002). Mutant cells were characterized by the presence of an anomalous accumulation of Tdp1–DNA complexes, which, together with the stalled topo I-DNA complexes, negatively affected transcription. Tdp1 can also process protruding 3′-phosphoglycolate termini on DNA double-strand breaks formed in response to oxidative stress (Inamdar et al. 2002). In addition, Interthal et al. (2001) demonstrated that Tdp1 is able to cleave a phosphoamide bond. All these reports support the additional cellular functions of the Tdp1 enzyme, besides its role in the repair of topo I-mediated DNA damage. In animal cells, Tdp1 is a member of the base-excision repair (BER) complex (El-Khamisy et al. 2005).

Despite the increasing body of literature dealing with Tdp1 in animal systems, no information on this enzyme are currently available in plants. Due to their sessile lifestyle, plants are continuously exposed to harmful genotoxic environmental conditions, which cause overproduction of reactive oxygen species (ROS), affecting crop quality and productivity. Within this context, the search for and the characterization of novel functions involved in the plant antioxidant response, particularly in the nuclear compartment, are required. Up to now, the transcriptional studies on stress-responsive genes have evidenced the complexity of mechanisms underlying signal sensing and transduction under oxidative stress conditions.

In plants, the response to the genotoxic effects induced by ROS involves activation of different DNA repair pathways having basic features in common with those found in animals (Kimura and Sakaguchi 2006). However, several DNA repair genes are present in multiple copies in plant genomes and this seems to suggest that the presence of multiple alleles might increase tolerance to oxidative damage. Moreover, differently from animals, some of the plant genes involved in the nucleotide-excision repair (NER) and BER pathways might also participate in other processes, correlated with cell cycle control and transcription regulation (Kimura and Sakaguchi 2006).

It is reasonable to hypothesize that the strict relationship between the Tdp1 and topo I enzymes, evidenced in animal cells, might also exist in plants. Although the essential role played by topo I in proliferation events occurring during plant growth and development has been demonstrated (Singh et al. 2004), several questions concerning other topo I functions in planta remain still open.

The presence of two functional *top1* loci in a eukaryotic organism was demonstrated for the first time in *Daucus carota* (Balestrazzi et al. 2000). To investigate the relationship existing between the topo I-mediated DNA damage and other intracellular pathways involved in the defense response, transgenic cell lines showing antisense-mediated depletion of the *top1β* gene expression were produced and analyzed (Locato et al. 2006). Since another intriguing point, still uncovered in plants, is related to the involvement of topo I in DNA repair, the parallel investigation of *Tdp1* and *top1* genes might produce useful information.

The extensive bioinformatic and database resources, currently available for the model legume *Medicago truncatula*, facilitate the studies of relevant biological processes controlled by genes so far not fully characterized. For this reason, *M. truncatula* might represent a valuable tool to expand the knowledge on DNA repair mechanisms. Notwithstanding the recent advances in the study of DNA repair in higher plants, deeper investigation is still required, considering the harmful effects caused on genomes by environmental deterioration. The present study, carried out using barrel medic (*Medicago truncatula* Gaertn.), describes for the first time in plants the *Tdp1* genes encoding tyrosyl-DNA phosphodiesterase. The main goal of our research was to assess the expression profiles of *Tdp1* genes in barrel medic in response to stress induced by copper and PEG, respectively, in view of their possible use for in planta overexpression studies. The latter will help defining the potential of *Tdp1* genes as tools able to make plants tolerant to adverse environmental conditions.

Materials and methods

Plant material

Medicago truncatula Gaertn. (genotype R108-1), used in this study, was selected by Trinh et al. (1998) due to its high embryogenic potential and genetic trasformation

properties. In vitro plantlets were grown in sterile containers (Micropoli, Cesano Boscone, Italy) on a medium containing macrosalts and microsalts MS (Murashige and Skoog 1962), vitamin SH (Schenk and Hildebrandt 1972), 20 g l^{-1} sucrose and 4 g l^{-1} gerlite (Duchefa Biochemie, Haarlem, The Netherlands). They were maintained in a climate chamber at 22–24°C with a 16-h light/8-h dark cycle photoperiod and a photosynthetic photon flux of 65–70 μmol m^{-2} s^{-1} under a cool white fluorescence lamp. For oxidative stress treatments, copper and polyethylene glycol (PEG 6000; Duchefa Biochemie) were added at the indicated concentrations (0, 0.05, 0.1 and 0.2 mM CuCl$_2$; 0, 50, 100 and 150 g l^{-1} PEG 6000). The water potential of the culture medium was estimated at -0.30 MPa (0 g l^{-1} PEG 6000), -0.60 MPa (50 g l^{-1} PEG 6000), -0.66 MPa (100 g l^{-1} PEG 6000) and -1.0 MPa (150 g l^{-1} PEG 6000). For imbibition experiments, seeds obtained from plants grown in greenhouse were transferred to Petri dishes (9 cm diameter; 100 seeds per dish) with two filter papers moistened with 2.5 ml distilled water and kept in a growth room at 22°C under a photoperiod of 16/8 h, photon flux density of 150 μmol m^{-2} s^{-1} and a relative humidity (RH) of 70–80%. For molecular analyses, plant tissues and seeds were collected at the indicated time points, the fresh weight was measured and samples were then stored in liquid N$_2$.

Bioinformatic analysis

The search for the nuclear localization signal was carried out using NucPred (http://www.sbc.su.se/~maccallr/nucpred/cgi-bin/single.cgi; Brameier et al. 2007). Nucleotide and amino acid sequences were obtained from http://www.ncbi.nlm.nih.gov/entrez/viewer.fcgi (*A. thaliana* and *P. trichocarpa*) and http://compbio.dfci.harvard.edu/tgi/ (*M. truncatula*). The program CLUSTALW (http://www.ebi.ac.uk/tools/clustalw2/index.html) was used to create the alignments. The search for sumoylation sites was carried out at: http://www.abgent.com/tools/sumoplot.

Biomass production, copper measurement, chlorophyll estimation and analysis of free proline content

To evaluate the effects of oxidative stress treatments on plant growth and biomass production, the fresh weight of aerial parts and roots from untreated (control) and treated in vitro plantlets was measured 30 days after the beginning of the experiment. For each treatment, nine replications of single-plantlet experimental units were analyzed. Three in vitro plantlets were grown in each container. The average biomass values of roots and aerial parts per container were expressed in mg ± standard deviation. For copper determination, plantlets grown for 30 days in the presence/absence of 0.2 mM CuCl$_2$ were harvested and dried in an oven at 60°C for 5 days for dry weight measurements. The chemical analyses (by Idrocons s.r.l., Rivalta Scrivia, Tortona, Italy) were carried out by ICP-OES (inductively coupled plasma optic emission spectrometry) using an IRIS Advantage ICAP DUO HR series (Thermo Jarrell Ash, Franklin, MA, USA) spectrometer. The chlorophyll content of plantlets was determined 10, 20 and 30 days after exposure to copper (0.2 mM CuCl$_2$) and PEG 6000 (150 g l^{-1}), respectively. Untreated plantlets were also evaluated. Fresh leaves (0.5 g) were homogenized using a pestle and mortar in 3 ml of 80% acetone. The homogenate was centrifuged (1,957g) and the resulting supernatant was used for chlorophyll estimation. Absorbance of the solution was measured at 645 and 663 nm, using a V-530 spectrophotometer (Jasco Europe S.r.l., Cremella, Italy). Chlorophyll a, chlorophyll b and total content were calculated according to the following formulas: $C_a = 12.72 A_{663} - 2.59 A_{645}$, $C_b = 22.88 A_{645} - 4.67 A_{663}$, $C_T = 20.29 A_{645} + 8.05 A_{663}$ (Wellburn 1994). Proline was determined according to the procedure described by Bates et al. (1973). Aerial parts and roots (500 mg) from 30-day-old untreated and treated in vitro plantlets were extracted with 3% aqueous 5-sulphosalicylic acid, centrifuged at 1,957g. The resulting supernatant was used for the proline assay and measured at 520 nm. Proline content was expressed as mmol g^{-1} fresh weight.

ROS detection

Detection of reactive oxygen species (hydrogen peroxide and the superoxide radical) was carried out using the specific dyes 3,3′-diaminobenzidine (DAB, Sigma–Aldrich, Milan, Italy) and nitroblue tetrazolium (NBT, Sigma–Aldrich), as described by Thordal-Christensen et al. (1997) and Fryer et al. (2002), respectively. For each treatment, three plantlets were analyzed. Quantitation of dark areas was performed using a Biostep GmbH apparatus with the argus X1 3.3.0 software.

Evaluation of DNA damage

To evaluate the level of 7,8-dihydro-8-oxoguanine (8-oxo-dG), DNAs were extracted from leaf tissues of treated and untreated plantlets and from germinating seeds, as described by Rogers and Bendich (1989) with the following modifications: deproteinization was carried out only once using chloroform/isoamyl alcohol to avoid undesired oxidation effects due to phenol treatment. Purified DNAs were digested with proteinase K (10 mg ml^{-1}, Sigma–Aldrich) for 2 h at 37°C according to the supplier's suggestions and subsequently deproteinized as previously described. Hydrolysis was carried out by incubating barrel medic DNA (100 μg) with DNase I (10 μg, Sigma–Aldrich) for 12 h at 37°C, followed by treatment with alkaline phosphatase

(10 units, M-Medical S.r.l., Cornaredo, Italy) for 2 h at 37°C. Free deoxynucleosides were then purified by filtration using Vivaspin 500 (VivaScience, Sartorius; Sigma–Aldrich). Detection and quantification of 8-oxo-dG in DNA samples was carried out using the New 8-OHdG Check Trial Kit (JalCA, Shizuoka, Japan) according to the manufacturer's instructions.

RNA extraction, cDNA synthesis and quantitative real-time polymerase chain reaction

RNA extraction was carried out with the NucleoSpin RNA II Extraction Kit (Macherey–Nagel, Düren, Germany; M-Medical S.r.l.), according to the supplier's suggestions. Total RNA was then quantified by agarose gel electrophoresis and spectrophotometric analysis as indicated by Sambrook et al. (1989). Total RNA was reversely transcribed into cDNAs using the High Capacity cDNA Reverse Transcription kit (Applied Biosystems International, Monza, Italy), as indicated by the supplier. Quantitative real-time polymerase chain reaction (QRT-PCR) was carried out in 15 µl, using the QuantiTect SYBR Green PCR kit (Qiagen S.p.A., Milan, Italy) and a Rotor-Gene 6000 PCR apparatus (Corbett Robotics Pty Ltd, Brisbane, Queensland, Australia). A barrel medic tubulin gene (C7068808) was used as standard control in the RT-PCR reactions (Brunner et al. 2004). To analyze the expression profiles of barrel medic *MtTdp1α* (AC122166), *MtTdp1β* (AC141864.7), *top1α* (CA919655), *top1β* (CX526330) and *APX* (DY616600) genes, the oligonucleotide primers were designed using the Real-Time PCR Primer Design program from GenScript (Table 1). An amplicon size of ∼100 bp was targeted to obtain efficient amplification (Bustin 2000). QRT-PCR conditions were as follows: denaturation at 95°C for 15 min, and cycling at 94°C (15 s), 55°C (30 s) and 72°C (30 s). For each primer set, a no-template water control was used. The QRT-PCR results were interpreted using the LinRegPCR computer software (Ramakers et al. 2003). For each set of PCR reactions, the logarithms of the initial fluorescence (No) was calculated based on the individual PCR

efficiency. The logarithm of relative fluorescence unit (Log-RFU) was used for graphic representation.

Statistical analysis

For each experiment, three replicated plants from each treatment combination were randomly selected for biochemical and molecular analyses. Results were subjected to analysis of variance (ANOVA) and the statistical significance of mean differences was determined using Tukey's test.

Results

The barrel medic *Tdp1* gene family

The search for a *Tdp1* sequence in barrel medic databases revealed the presence of a small gene family composed of two members (hereby named *MtTdp1α* and *MtTdp1β* encoding two distinct isoforms of tyrosyl-DNA phosphodiesterase (*Mt*Tdp1α and *Mt*Tdp1β). The deduced amino acid sequence of the *Mt*Tdp1α protein is shown in Fig. 1. The open reading frame (ORF) encodes a protein of 634 amino acids (aa) with a putative molecular mass of 71.3 kDa. The *Mt*Tdp1α N-terminal region contains a putative nuclear localization signal (NLS) composed of a short cluster of basic amino acid residues (KRRK; Fig. 1, aa 82–85). Two HKD motifs (HKD-I, aa 261–291; HKD-II, aa 491–516), located within the N-terminal and within the C-terminal regions, respectively, were identified (Fig. 1). Three motifs (LKWP, aa 326–329; LKPG, aa 545–548; FKKD, aa 623–626), typical of sumoylation sites, were detected within the *Mt*Tdp1α protein (Fig. 1). The deduced amino acid sequence of the *Mt*Tdp1β protein is shown in Fig. 2. The ORF encodes a protein of 1064 amino acids with a putative molecular mass of 119.1 kDa. The *Mt*Tdp1β N-terminal region contains a putative nuclear localization signal (NLS), which includes the basic amino acid residues KRRKR (Fig. 2, aa 207–211). In the *Mt*Tdp1β protein, two

Table 1 Sequences of oligonucleotide primers utilized in QRT-PCR

Gene	Forward primer	Reverse primer	Efficiency[a]
Tdp1α	5′-ACGAGTTGGGAGTGCTCTTT-3′	5′-GGGATTTATCCTTCGATTGTTT-3′	1.72
Tdp1β	5′-GGTTGGTTTGAGCCATCTTT-3′	5′-GCAGGCACATTGTGATTTCT-3′	1.79
top1α	5′-AAACTGACATCGGGAGGAAC-3′	5′-TTCTGCTTCACCCAGTCATC-3′	1.60
top1β	5′-ATACACGTGGGCTATTGTCG-3′	5′-TCACTTGGATGAATGCGTT-3′	1.67
APX	5′-AGCTCAGAGGTTTCATCGCT-3′	5′-CGAAAGGACCACCAGTCTTT-3′	1.80
TUB	5′-GGAATGGAGGATCCGAATAA-3′	5′-CCTGTTGCTTGTCACTTGGT-3′	1.80

[a] Efficiency of the primer pair in QRT-PCR

Fig. 1 *Mt*Tdp1α amino acid sequence (ABE78603). The putative nuclear localization signal (KRRK) is represented in *bold* within a *gray box*. The HKD motifs (I and II) are indicated in *bold* with the most conserved amino acids *underlined*. The putative sumoylation sites (LKWP, LKPG, FKKD) are represented in white within *dark gray boxes*

```
  1  MSFSHSQIGYLIPLNPNSEEKEKASTPKLTISDGTNIIGRNNVPVNDKRL   50

 51  SRKHLTITASADGTANLHVEGTNPVVVNSGNKRRKLNSKQTAAIFDGDVI  100

101  ELIPGHYLFKYQVSQRSPKVADNKHHERGKNSATQRHDKIAVTQKHGSSR  150
151  SCEEPIRDFRVADDQIPCTFRLLRVQGLPPWANTSCVSISDVIQGDILVA  200
201  VLSNYMVDVDWLVPACPALSKVPHVLVLHGESDERVACIKRSKPKNWILH  250
                        HKD motif-I
251  KPPLPISFGTHHSKAMFLVYPRGVRVIIHTANLIYVDWNNKSQGLWMQDF  300

301  PWKDQNSPSKGSRFENDLVEYLSALKWPEFSVNLPSLGNFSICPSFFKKF  350

351  DYSDAMVRLIASVPGYHSGNGLKKWGHMKLRSVLQECTFDKEFKKSPLVY  400
401  QFSSLGSLDEKWMVELASSMSAGLSEDKVPLGMGEPQIIWPTVEEVRCSI  450
451  EGYAAGSAIPSPMKNVEKAFLKKYWAKWKANHTGRTRAMPHIKTFARYNN  500
                                            HKD motif-II
501  QNLAWFCLTSSNLSKAAWGALQKNNSQLMIRSYELGVLFLPSLLKPGCGF  550

551  SCTSNVKQSKDKSPAQETSKMKKTKLVTLTAPTRDTTHSSSEVIIQLPVP  600

601  YELPPLPYSSEDVPWSWDRRYFKKDDYGQVWPRM                 634
```

Fig. 2 *Mt*Tdp1β amino acid sequence (ABE85647.1). The putative nuclear localization signal (KRRKR) is represented in *bold* within a *gray box*. The HKD motifs (I and II) are indicated in *bold* with the most conserved amino acids *underlined*. The putative sumoylation site (LKNG) is represented in white within *dark gray boxes*

```
   1  MIDSNSNSNHNKRPFPHIPLSSVSVVLNHFHLPLFSTSQNGIVSLCTTMH    50
  51  LHADQPYSIGRKRHDCHFVFNDRRVSKRHCQIFFDGSLRKLYILSGILSN   100
 101  TGSAIDSKSRIVHEFRKRVMMFSCGSEGFPILEASNGVFVNGVEIRKGMA   150
 151  VELMEGDRVSLVCGNWNASCGIGNRIGFVVDRIIVENCNGVGGIDGSTFS   200

 201  GHSQSDKRRKRVFAVKANDSKFDGVFVRAKYLIDRCRDILLSHDPLSCIL   250

 251  HSDSDLQCGYKFEIGTELAQRAREDTGIDVVQSSSGLLCKSKGIDLEENG   300
 301  ENFCRKGDLGVDYVNAFGDKNLNLTVSDSIEKDNVSSDSDNEQGTNQHDF   350
 351  YPPPGKNFYLNRLEYMNHDSSSGLDNSISLTELIHPIESVTRMFIATFTS   400
 401  DITWFLTYCKIPYHLPVTIACQNTEKCWSSKPDERVFVPYQNYPNLVVVH   450
                                            HKD motif-I
 451  PPFPETIAFGKDHKRHGIACHHPKLIVLQREDSIRVIITSANLVEKQWNS   500

 501  VTNTIWWQDFPRAILVDYASLFRKIDDDEVHRNSKCDFAAQLAGFMASLV   550
 551  IDVPSQAHWITQLTKYDFGSATGHLVASLPGIHLNRTSVLLESFQSSSFL   600
 601  GSVVASVVGLSHLFRAVADSNSAGLRALAAVLGKYCKNVNGRFEIVLRRN   650
 651  HNVPADENAVSVLVPKSDQTSEGDFVQLGFLPRNLAKWVSPLWDAGFFSF   700
 701  SGYVCPKEALAAALGENSQKLQLILNVSEGHHFRDMSKMMQSEQIAAFCS   750
 751  LIASIQRHYGLWRLQEVLNQYRWPESLESEIVYGASSIGSVNSKFLAAFS   800

 801  AAAGKKSLQHFDSEESDPEWGCWNAREELKNPSVKIIFPTIERVKSAYNG   850

 851  ILPSRRILCFSERTWQRLKTLDVLHDAVPHPHERVGHPMHTKVVRRCFWS   900
            HKD motif-II
 901  RGEAPSIGWVYCGSHNFSAAAWGRQISNPFGTKADDPHKGDPSVNSGLHI   950

 951  CNYELGIIFTFPPSENNECPKVKSTKLDDIVLPYVVPAPKYGSLDKPATK  1000
1001  LAMREVMTELAEREGEKQAEEEIMEEILEEEEEIEEINCVGEEKEEEKAY  1050
1051  AEILWSQVDSSQNS                                     1064
```

HKD motifs (HKD-I, aa 471–499; HKD-II, aa 890–923), located within the central region and within the C-terminal domain, respectively, were identified (Fig. 2). The motif LKNP (aa 829–832) typical of sumoylation sites was also detected (Fig. 2). The comparison between the amino acid sequences of *Mt*Tdp1α and *Mt*Tdp1β isoforms revealed a low level (18.79%) of similarity (data not shown).

A search for *MtTdp1α* and *MtTdp1β* gene homologs, carried out in other plant databases, confirmed the existence of a small *Tdp1* gene family also in different species, such as *Arabidopsis thaliana* and *Populus trichocarpa*. Results are shown in Suppl. Fig. 1S. The comparison between the *Mt*Tdp1α amino acid sequence and the *A. thaliana* and *P. trichocarpa* Tdp1α sequences evidenced that the region

included between aa 258 and aa 556 of the *Mt*Tdp1α protein shares 77.18 and 82.20% similarity with the α isoform of *A. thaliana* and *P. trichocarpa*, respectively. The comparison between the *Mt*Tdp1β amino acid sequence and the *A. thaliana* and *P. trichocarpa* Tdp1β sequences is shown in Suppl. Fig. 2S. The region included between aa 469 and aa 957 of the *Mt*Tdp1β protein shows 41.59 and 69.19% similarity with the β isoform of *A. thaliana* and *P. trichocarpa*, respectively. It is worth noting that the presence of a small *Tdp1* gene family has been identified in several other plant species, including rice (*Oryza sativa*) and wheat (*Triticum aestivum*) (data not shown). The comparison between the amino acids sequences of *Mt*Tdp1α and *Mt*Tdp1β isoforms and the human Tdp1 sequence revealed a similarity of 27.70 and 18.92%, respectively. All the plant Tdp1α isoforms analyzed in this study ranged in size from 67.2 to 71.3 kDa, similarly to the human Tdp1 (66.0 kDa).

Alignment of the HKD motifs found in the human Tdp1 protein with the HKD motifs of the plant Tdp1α and β isoforms, analyzed in this study, is shown in Suppl. Fig. 3S. As evidenced in the figure, the most conserved amino acids (histidine, lysine and asparagine) were present in all the plant Tdp1 isoforms. As for the HKD motif-I of the plant Tdp1α protein, the histidine residues His-261 (*M. truncatula*), His-236 (*A. thaliana*) and His-267 (*P. trichocarpa*) correspond to the His-263 catalytic residue of the human Tdp1 enzyme (Suppl. Fig. 3S, a). Similarly, within the HKD motif-II of the plant α isoform, the histidine residues His-490 (*M. truncatula*), His-465 (*A. thaliana*) and His-498 (*P. trichocarpa*) correspond to the conserved H-493 residue of the human protein (Suppl. Fig. 3S, a). In both HKD motifs there are also conserved lysine residues (Lys-263 and Lys-492, *M. truncatula*; Lys-238 and Lys-467, *A. thaliana*; Lys-270 and Lys-500, *P. trichocarpa*) corresponding to the Lys-265 and Lys-295 residues of the human protein (Suppl. Fig. 3S, a). Similar features are also found in the plant β isoform (Suppl. Fig. 3S, b). Within the HKD motif-I of the plant Tdp1β protein, the histidine residues His-472 (*M. truncatula*), His-475 (*A. thaliana*) and His-488 (*P. trichocarpa*) correspond to the His-263 catalytic residue of the human Tdp1 enzyme (Suppl. Fig. 3S, b). When considering the HKD motif-II of the plant β isoform, the histidine residues His-891 (*M. truncatula*), His-897 (*A. thaliana*) and His-900 (*P. trichocarpa*) correspond to the His-493 conserved residue of the human protein (Suppl. Fig. 3S, b). As previously reported for the α isoform, in both HKD motifs of the plant Tdp1β protein there are conserved lysine residues (Lys-474 and Lys-893, *M. truncatula*; Lys-477 and Lys-899, *A. thaliana*; Lys-490 and Lys-902, *P. trichocarpa*), corresponding to the Lys-265 and Lys-295 residues of the human protein (Suppl. Fig. 3S, b).

Another distinctive feature of the Tdp1 protein is the presence of a DNA-binding groove, which interacts with single-strand DNA by means of three key serine residues, namely Ser-400, Ser-403 and Ser-518 in the case of human Tdp1. In the Tdp1α isoform, there are conserved serine residues located in regions having high similarity with the human sequence (Suppl. Fig. 4S, a). Those residues were identified in *M. truncatula* (Ser-404, Ser-407 and Ser-514), *A. thaliana* (Ser-379, Ser-382 and Ser-489) and *P. trichocarpa* (Ser-411, Ser-414 and Ser-521; Suppl. Fig. 4S, a). The search for the key DNA-binding residues in the β isoform allowed to detect only a serine (Ser-918, *M. truncatula*; Ser-927, *A. thaliana*; Ser-928, *P. trichocarpa*), corresponding to the Ser-518 of human Tdp1 (Suppl. Fig. 4S, b). No other serine residues are present in the β isoform since phenylalanine (Phe-680, *M. truncatula*; Phe-687, *A. thaliana*; Phe-699, *P. trichocarpa*) and glutamine (Gln-677, *M. truncatula*; Gln-684, *A. thaliana*; Gln-696, *P. trichocarpa*) replace the Ser-400 and Ser-404 residues of the human protein (Suppl. Fig. 4S, b).

Response to copper and PEG in barrel medic plantlets grown in vitro

Medicago truncatula plantlets were grown in vitro for 30 days with increasing copper doses (0.05, 0.1 and 0.2 mM $CuCl_2$) and in the absence of heavy metal. The toxic effects of copper on the growth rate were visible at all the tested concentrations (data not shown), but root elongation and development of the aerial parts were remarkably inhibited by the highest copper dose, compared to untreated plants (Fig. 3a, b). In the absence of heavy metal, the average biomass values of roots and aerial parts per container were 587 ± 2 and $1,112 \pm 5$ mg, respectively. After 30 days of exposure to the highest copper dose, the average fresh weight of roots and aerial parts per container were significantly ($P < 0.0001$ and $P < 0.0001$, respectively) reduced, corresponding to 0.084 ± 0.004 and 0.371 ± 0.002 mg, respectively.

The copper amounts in untreated plants were 3.70 mg kg^{-1}dry weight (roots) and 2.65 mg kg^{-1}dry weight (aerial parts), respectively. After 30 days of treatment (0.2 mM $CuCl_2$), the heavy metal content was 924 mg kg^{-1}dry weight (roots) and 104 mg kg^{-1}dry weight (aerial parts), respectively.

Similarly, the PEG 6000 treatment (50, 100 and 150 g l^{-1}) strongly limited the in vitro growth of barrel medic plants. The effects caused by the highest PEG 6000 concentration are visible in Fig. 3c. After 30 days of treatment with PEG 6000 (150 g l^{-1}), the average fresh weight of roots and aerial parts per container were significantly ($P < 0.0001$ and $P < 0.0001$, respectively) affected, compared to the untreated tissue and were estimated at 166.7 ± 3.5 and 74.3 ± 2.5 mg, respectively.

Across time sampling, the treatment with 0.2 mM $CuCl_2$ caused significant ($P < 0.0001$) effects on the total chlorophyll
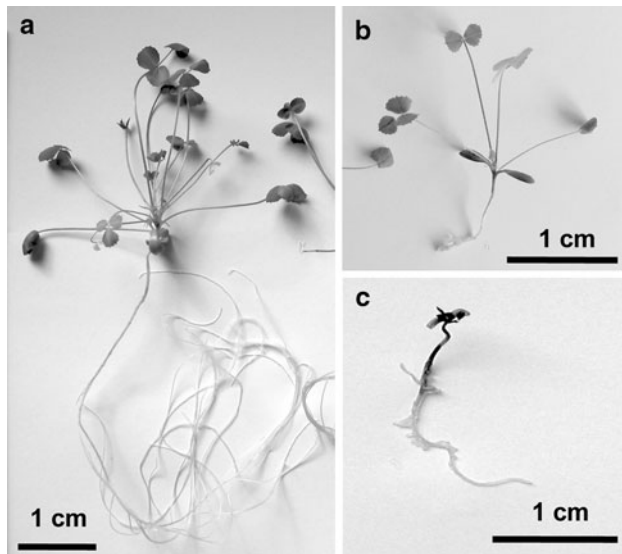
Fig. 3 Thirty-day-old barrel medic plantlets grown in vitro in the absence of stress (**a**), in the presence of 0.2 mM CuCl$_2$ (**b**) and in the presence of 150 g l^{-1} PEG (**c**)

content. Ten days following exposure to 0.2 mM CuCl$_2$, the total chlorophyll amount was approximately 2.1-fold the value measured for the untreated tissues and it only slightly changed (1.6- and 1.9-fold) at 20 and 30 days, respectively (Suppl. Fig. 5S). The exposure to copper caused a significant ($P = 0.0001$) increase in free proline content only in the aerial parts (Suppl. Fig. 5S). Across time sampling, the treatment with PEG 6000 (150 g l^{-1}) caused significant ($P < 0.0001$) effects on the total leaf chlorophyll content. Ten days following exposure to PEG 6000, the total chlorophyll amount was approximately 2.9-fold the value measured for the untreated tissues and it further increased (9.4-fold) at 20 days (Suppl. Fig. 5S). As for free proline content, the analysis of variance revealed significant ($P < 0.0001$) differences between untreated and PEG 6000-treated plant tissues at the end of the treatment period.

ROS accumulation in response to copper and PEG treatments

Accumulation of endogenous hydrogen peroxide (H$_2$O$_2$) in leaves of 30-day-old plantlets grown in vitro on increasing copper concentrations was detected in situ by treatment with 3,3′-diaminobenzidine (DAB), while the level of superoxide radical (O$_2^-$) was evaluated using nitroblue tetrazolium (NBT). Results from these experiments are shown in Fig. 4. Staining was absent from the leaf tissue of untreated barrel medic plantlets (Fig. 4, a-DAB and b-NBT, NT), while the ROS-specific brown and blue precipitates were clearly visible in the stressed samples (Fig. 4, a-DAB and b-NBT, 0.2 mM CuCl$_2$ and PEG, 150 g l^{-1}). The analysis of variance revealed significant differences
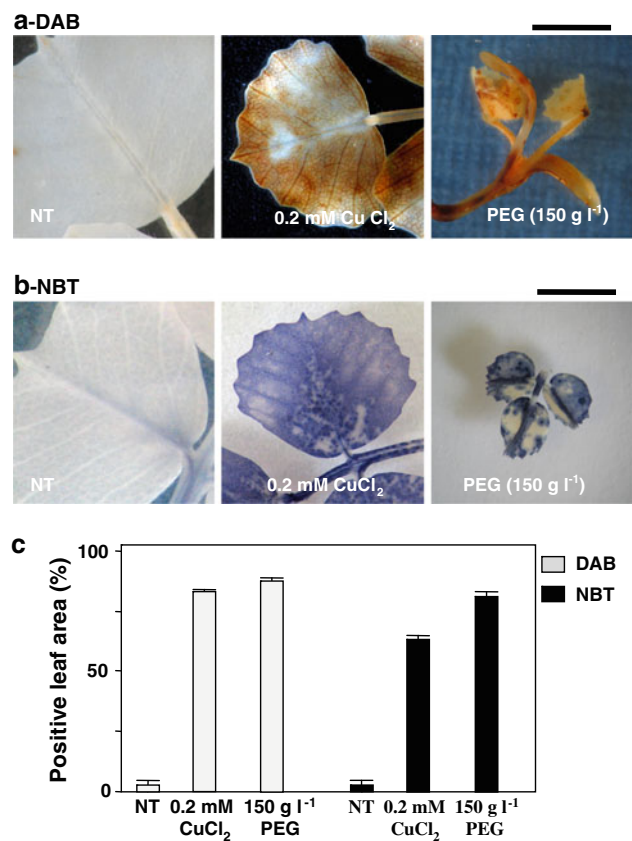

Fig. 4 Accumulation of endogenous hydrogen peroxide (H$_2$O$_2$) and superoxide radicals (O$^-$) in leaves of 30-day-old plants grown on copper and PEG. **a** DAB-stained leaf tissue. **b** NBT-stained leaf tissue. **c** Quantitation of *dark areas* allowed to quantify the amount of ROS accumulation. For each treatment, data were derived from three independent replications

($P < 0.0001$) among treatments for the percentage of DAB- and NBT-stained leaf areas, respectively. The percentage of DAB- and NBT-stained leaf areas from untreated plantlets was 2% and was significantly ($P = 0.0001$) different from the copper and PEG 6000-treated barrel medic plantlets, according to Tukey's test. Thirty days after treatments, the percentage of DAB-stained leaf areas was quantified at 82.3% in case of 0.2 mM CuCl$_2$ and 84% in case of 150 g l^{-1} PEG 6000 (Fig. 4c). As far as the percentage of NBT-stained leaf areas is concerned, Tukey's test revealed a significant increase in the level of superoxide radical (O$_2^-$) between copper and PEG 6000-treated barrel medic plantlets: the percentage of NBT-stained leaf areas was quantified at 70.7% in case of 0.2 mM CuCl$_2$ and 82.3% in case of 150 g l^{-1} PEG 6000 (Fig. 4c).

Oxidative DNA damage in leaf tissues exposed to copper and PEG treatments

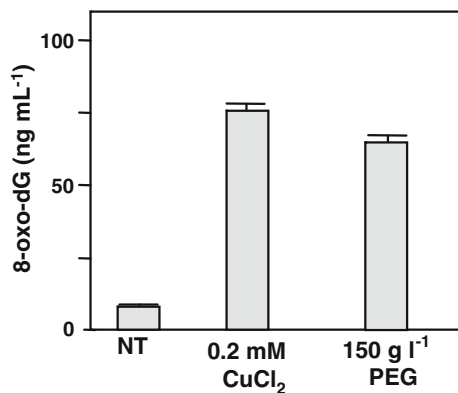The level of DNA damage in leaves of plantlets challenged with oxidative stress was determined using a commercially

Fig. 5 DNA damage as revealed by the level of 8-oxo-dG in DNAs extracted from the aerial parts of untreated plants (NT) and plants exposed to 0.2 mM $CuCl_2$ and 150 g l^{-1} PEG. The levels of 8-oxo-dG were evaluated by an ELISA assay. The range of assay's calibration curve was 0.50–120.00 ng ml^{-1}. For each treatment, data represent the mean values of three independent replications

available ELISA kit (Fig. 5). When DNA extracted from untreated plantlets was evaluated, the amount of 8-oxo-dG was estimated on average as 10.33 ± 1.53 ng ml^{-1}, corresponding to 9.34×10^2 8-oxo-dG/10^5 dG. The low level of oxidative DNA damage was in agreement with the parallel evaluation of the stress parameters reported for the untreated tissues in the previous paragraphs. Tukey's test revealed a significant ($P = 0.0001$) increase in the level of DNA damage detected in plants exposed for 30 days to copper (0.2 mM $CuCl_2$) and PEG 6000 (150 g l^{-1}) when compared with the untreated plants. In response to copper, a value of 77.0 ± 2.65 ng ml^{-1} corresponding to 72.82×10^2 8-oxo-dG/10^5 dG was observed, while in the PEG 6000-treated sample the estimated amount was 70.00 ± 5.10 ng ml^{-1}, corresponding to 66.38×10^2 8-oxo-dG/10^5 dG (Fig. 5). The level of oxidative DNA damage in those tissues exposed to oxidative stress increased up to 7.4- and 6.7-fold in case of copper and PEG 6000 treatments, respectively.

The barrel medic *MtTdp1* and *top1* genes are up-regulated in the presence of copper

The expression profiles of *MtTdp1α* and *MtTdp1β* genes, encoding the α and β isoforms of barrel medic tyrosyl-DNA phosphodiesterase, were evaluated in plantlets grown in vitro for 30 days in the presence/absence of copper (0, 0.05, 0.1 and 0.2 mM $CuCl_2$; Fig. 6). As far as *MtTdp1α* average expression level in aerial parts is concerned, Tukey's test revealed a significant ($P = 0.02$) increase in the average amount of the target mRNA of 0.2 mM $CuCl_2$-treated plantlets, when compared with the untreated tissues. The analysis of variance revealed no significant ($P = 0.97$) differences among treatments in the average level of the
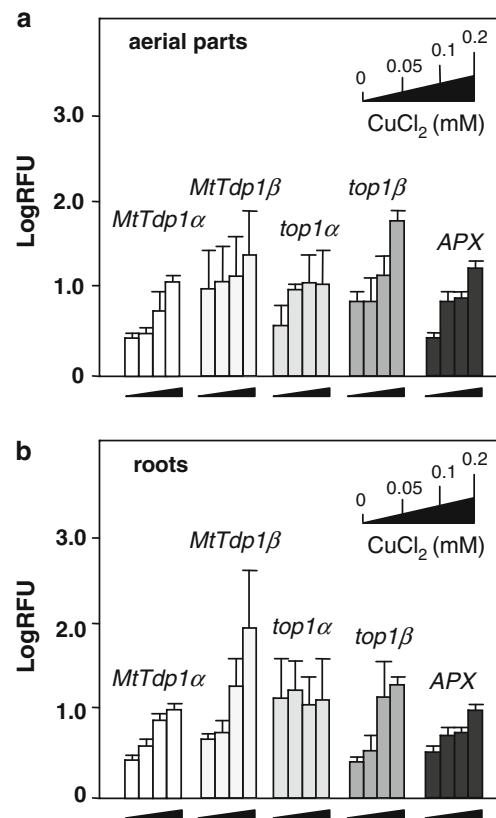

Fig. 6 Results from QRT-PCR analyses carried out on aerial parts (**a**) and roots (**b**) of barrel medic plants grown in vitro for 30 days in the presence/absence of increasing copper doses. For each treatment combination, data represent the mean values of three independent replications

MtTdp1β transcript. In the aerial parts, the highest *MtTdp1α* and *MtTdp1β* expression levels were detected in response to 0.2 mM $CuCl_2$. The up-regulation of *MtTdp1α* and *MtTdp1β* genes resulted in 2.1- and 1.3-fold the values measured for the untreated tissues (Fig. 6a). Tukey's test revealed a significant ($P = 0.0001$ and $P = 0.04$, respectively) increase in the average amount of *MtTdp1α* and *MtTdp1β* transcripts in the roots of 0.2 mM $CuCl_2$-treated plantlets when compared with the untreated tissues. At the highest copper dose, the up-regulation of *MtTdp1α* and *MtTdp1β* in the roots was estimated at 1.9- and 3.2-fold, respectively (Fig. 6b).

The expression profiles of *top1α* and *top1β* genes, encoding the α and β isoforms of barrel medic DNA topoisomerase I, were also evaluated in plantlets exposed to copper. As far as *top1α* average expression level in aerial parts is concerned, the analysis of variance was not significant ($P = 0.60$) among treatments. Tukey's test revealed a significant ($P = 0.05$) increase in the average amount of *top1β* transcript in the aerial parts of 0.2 mM $CuCl_2$-treated plantlets, when compared with the untreated tissues. In the aerial parts, the up-regulation of *top1α* and *top1β* genes resulted

in 1.7- and 1.9-fold the values measured for the untreated tissues (Fig. 6a). As far as *top1α* expression level in roots is concerned, no significant ($P = 0.96$) differences among treatments were observed. The analysis of variance also revealed significant ($P = 0.04$) differences among treatments in the average level of the *top1β* transcript. In response to 0.2 mM $CuCl_2$, the up-regulation of *top1β* gene resulted in 3.2-fold the values detected for the untreated tissues (Fig. 6b).

As for *APX* (ascorbate peroxidase) gene expression in aerial parts, Tukey's test revealed a significant ($P = 0.0007$) increase in the amount of *APX* mRNA in the aerial parts of 0.2 mM $CuCl_2$-treated plantlets when compared with the untreated tissues, while in roots no significant ($P = 0.17$) differences among treatments were observed (Fig. 6a, b).

The *MtTdp1* and *top1* genes are responsive to PEG treatments

The expression profiles of *MtTdp1α* and *MtTdp1β* genes were evaluated in aerial parts and roots of plantlets grown in vitro for 30 days in the presence/absence of PEG 6000 (0, 50, 100 and 150 g l^{-1}; Fig. 7). Tukey's test revealed a significant ($P = 0.002$ and $P = 0.003$, respectively) increase in the average amount of *MtTdp1α* and *MtTdp1β* transcripts in the aerial parts of PEG 6000-treated plantlets when compared with the untreated tissues. The *MtTdp1α* and *MtTdp1β* gene expression levels gradually increased (up to 2.9- and 3.1-fold, respectively) in the aerial parts treated with increasing PEG 6000 concentrations (Fig. 7a). As far as the *MtTdp1α* average expression level in roots is concerned, the analysis of variance revealed significant ($P = 0.05$) differences in the level of the target mRNA among treatments. *MtTdp1α* showed a significant up-regulation (up to 1.6-fold) in the roots treated with the highest PEG 6000 concentration. In addition, the analysis of variance revealed significant ($P = 0.02$) differences in the average amount of *MtTdp1β* transcript among treatments. In the roots, the *MtTdp1β* expression level gradually increased in response to PEG treatments (Fig. 7b), and showed a significant ($P = 0.02$) up-regulation (2.2-fold) in plantlets exposed to 100 g l^{-1} PEG 6000.

The expression profiles of *top1α* and *top1β* genes were also evaluated in plantlets exposed to PEG 6000. The analysis of variance revealed no significant ($P = 0.48$) variation among treatments in the average amount of *top1α* transcript on aerial parts. According to Tukey's test, the *top1β* gene expression was significantly ($P = 0.02$) enhanced up to 2.6-fold in the aerial parts of barrel medic plantlets treated with the highest PEG 6000 concentration when compared with untreated tissues (Fig. 7a). For the *top1α* and *top1β* average expression levels in roots, no significant ($P = 0.68$ and $P = 0.43$, respectively) fluctuation of the target mRNAs
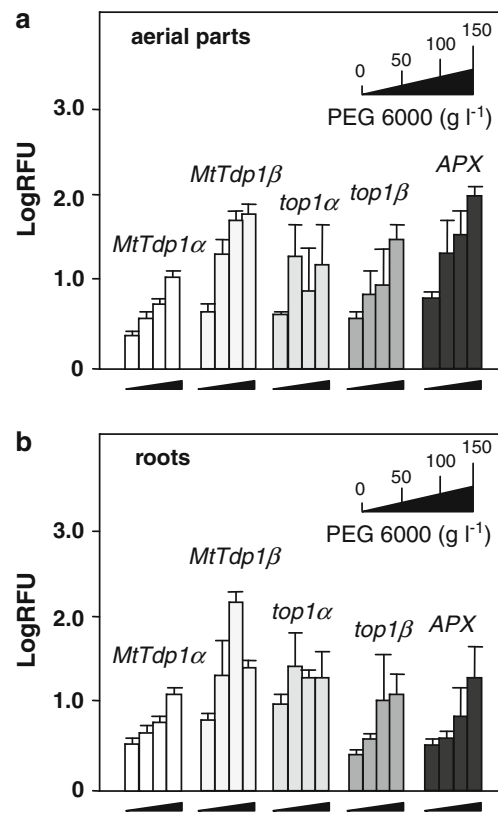

Fig. 7 Results from QRT-PCR analyses carried out on aerial parts (**a**) and roots (**b**) of barrel medic plants grown in vitro for 30 days in the presence/absence of increasing PEG concentrations. For each treatment combination, data represent the mean values of three independent replications

occurred in response to PEG treatments. In roots exposed to 150 g l^{-1} PEG 6000, the amount of *top1α* and *top1β* transcripts increased up to 1.4- and 2.0-fold, respectively, compared to the untreated sample (Fig. 7b).

For *APX* gene expression in aerial parts, the analysis of variance revealed significant ($P = 0.007$) differences among treatments in the level of the target mRNA. A significant ($P = 0.005$) increase in the average amount of *APX* transcript in response to the highest PEG 6000 concentration was detected, according to Tukey's test. No significant ($P = 0.15$) differences were detected among treatments for the *APX* gene expression in roots (Fig. 7a, b).

Both the *MtTdp1* and *top1* genes are up-regulated during seed rehydration

Due to the relevant role played by the animal *Tdp1* gene in DNA repair, the expression patterns of *MtTdp1* genes were investigated during seed imbibition, a process requiring active DNA repair. The phase 1 of imbibition was characterized by a rapid increase in fresh weight (from 0.3 to 0.85 g per 100 seeds), occurring during the first 8 h of rehydration (Fig. 8a). Between the 9 and 36-h period (phase 2 of

Fig. 8 **a** Increase in fresh weight occurring during barrel medic seed imbibition. **b** DNA damage as revealed by the level of 8-oxo-dG in DNAs extracted from barrel medic seeds at different times following rehydration. The levels of 8-oxo-dG were evaluated by an ELISA assay. The range of the assay's calibration curve was 0.50–120.00 ng ml^{-1}. For each sampling time, data represent the mean values of three independent replications. **c**, **d** Results from QRT-PCR analyses carried out on barrel medic seeds at different time points following rehydration. **e** Total *Tdp1* mRNA amounts. **f** Total *top1* mRNA amounts. For each treatment combination, values are expressed as the means of three independent replications
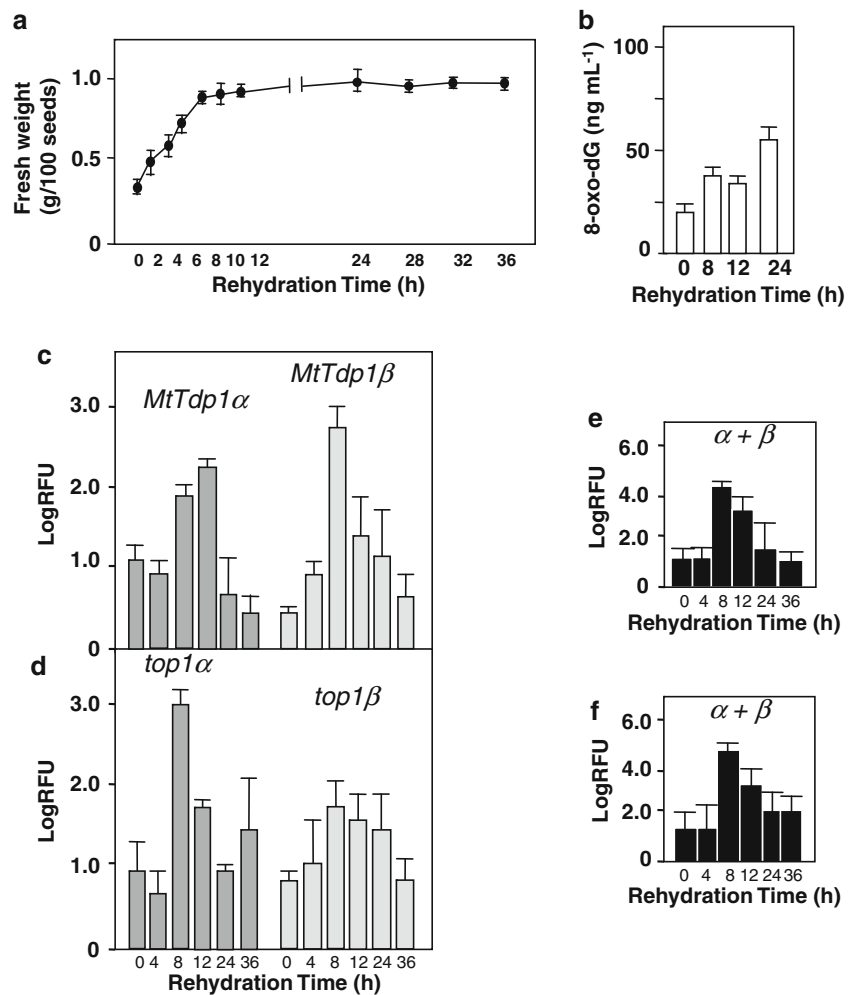
imbibition), no further increase in fresh weight was observed (Fig. 8a). The occurrence of oxidative DNA damage during seed imbibition was assessed by measuring the amount of 8-oxo-dG. As shown in Fig. 8b, at the beginning of the experiment (0 h), the estimated level of 8-oxo-dG was 21.67 ± 1.53 ng ml^{-1}, corresponding to 19.63×10^2 8-oxo-dG/10^5 dG. According to Tukey's test, a significant ($P = 0.0005$) increase (up to 42.00 ± 2.00 ng ml^{-1}, corresponding to 38.05×10^2 8-oxo-dG/10^5 dG and up to 39.33 ± 1.15 ng ml^{-1}, corresponding to 35.63×10^2 8-oxo-dG/10^5 dG) was observed at 8 and 12 h, respectively. Finally, the highest amount of 8-oxo-dG (52.67 ± 2.52 ng ml^{-1}, corresponding to 47.72×10^2 8-oxo-dG/10^5 dG) was detected in seeds at 24 h of rehydration (Fig. 8b).

Concerning the *MtTdp1α* expression level detected during seed rehydration, statistically significant ($P < 0.0001$) differences were observed among sampling time. A significant increase (1.8-fold) in the level of *MtTdp1α* mRNA was observed after 8 h of rehydration (Fig. 8c, *MtTdp1α*, 0 and 8 h). The average amount of *MtTdp1α* mRNA was still high (2.0-fold) at 12 h compared to the beginning of imbibition, while a decrease occurred at the end of the tested time

period (Fig. 8c, *MtTdp1α*, 36 h). The analysis of variance also revealed significant differences ($P = 0.0002$) among the different time points following rehydration for the average level of *MtTdp1β* transcript. The average amount of *MtTdp1β* mRNA detected at 8 h was significantly ($P = 0.04$) higher than that observed at other time points, according to Tukey's test. The *MtTdp1β* gene showed an up-regulation (5.5-fold) at 8 h of rehydration (Fig. 8c, *MtTdp1β*, 0 and 8 h). Then the amount of *MtTdp1β* mRNA decreased and, at the end of the experiment, almost reached the value recorded at 0 h (Fig. 8c, *MtTdp1β*, 36 h). Across *MtTdp1* genes, the analysis of variance also revealed significant differences ($P < 0.0001$) among the different time points following rehydration for the average level of *MtTdp1* transcript. According to the Tukey's test, the average amount of *MtTdp1* mRNA detected at 8 h was higher than that observed at 12 h, and significantly ($P = 0.005$) higher compared to that observed at other time points (Fig. 8e).

The *top1α* and *top1β* gene expression was also evaluated in barrel medic seeds during imbibition (Fig. 8d, f). The analysis of variance revealed significant differences ($P = 0.0015$) among the different time points following

rehydration for the average level of *top1α* transcript. A 3.0-fold up-regulation was observed after 8 h of rehydration (Fig. 8d, *top1α*, 0 and 8 h). Subsequently, a decrease in the level of *top1α* mRNA was detected, between 12 and 24 h, followed by a further enhancement occurring at 36 h (Fig. 8d, *top1α*). Concerning the *top1β* expression level detected during seed rehydration, no statistically significant ($P = 0.12$) differences were observed among sampling times. The *top1β* gene was up-regulated (1.9-fold) at 8 h of rehydration. The amount of *top1β* mRNA gradually decreased until the end of the experiment (Fig. 8d, *top1β*). Across *top1* genes, the analysis of variance also revealed a significant ($P = 0.0001$) variation in the average level of *top1* transcript among the rehydration times (Fig. 8f). The average amount of *top1* mRNA detected at 8 h was enhanced compared to that observed at 12 h and it was significantly ($P = 0.006$) higher compared to that observed for the other time points, according to the Tukey's test.

Discussion

In the present study and for the first time in a plant, the expression profiles of *Tdp1* gene encoding the DNA repair enzyme tyrosyl-DNA phosphodiesterase of the legume *M. truncatula* have been investigated under stress conditions. Differently from animals, where the *Tdp1* gene was found in single copy in the genome (Pommier et al. 2003), in this study the presence of a small gene family, not only in barrel medic but also in other plant species, was evidenced using bioinformatic tools.

As previously reported for the animal Tdp1 protein, both the *Mt*Tdp1α and *β* isoforms contain the two HKD motifs essential for the catalytic activity of the enzymes. The HKD motifs of Tdp1 orthologs from different species have been extensively investigated by Interthal et al. (2001). Due to the unique features of these motifs, the Tdp1 protein represents a member of a novel class of the phospholipase D superfamily (Interthal et al. 2001). The HKD motifs found in the plant protein contain the key histidine residues, which, in animals, have been demonstrated to catalyze the two sequential nucleophilic attacks required for the hydrolysis of the phosphodiester bond between a tyrosine residue and the phosphate group at the 3′ end of DNA (Yang et al. 1996). The HKD motifs of the plant Tdp1α and *β* isoforms also contain the conserved lysine residues, which form an anionic pocket between the histidine residues to anchor the phosphate. Based on the amino acid sequence alignments, the α isoform has more similarity with the human protein than the *β* isoform. Despite the low level of sequence conservation between the α isoform and the human Tdp1, both the components of the active site and those of the DNA-binding groove are present in

the plant Tdp1α protein. Within the putative DNA-binding region of the *β* isoform, the key serine residues are substituted by glutamine and phenylalanine, which can also interact with DNA bases.

Both the *Mt*Tdp1 isoforms contain a nuclear localization signal and some putative sumoylation sites. Sumoylation is a reversible post-translational modification catalyzed by the small-ubiquitin related modifiers (SUMOs). In animal cells, besides other physiological functions, sumoylation contributes to the regulation of several components of the DNA repair pathways. The nuclear localization of human XRCC4, a member of the nonhomologous end-joining (NHEJ) pathway, is determined by sumoylation (Yurchenko et al. 2006). To date, no reports on sumoylation of the Tdp1 protein in animal cells are available. The sumoylation system has been recently investigated in plants where it seems to be activated in response to biotic and abiotic stresses (Miura et al. 2007). The presence of putative sumoylation sites on the plant Tdp1 proteins suggests the possible involvement of such a mechanism in the regulation of Tdp1 function.

Investigation on the expression profiles of barrel medic *MtTdp1* genes revealed that both were constitutively expressed, thus confirming the basal requirement in planta for the two isoforms (data not shown). However, the main goal of the present work was the study of the expression profiles of *MtTdp1* genes in barrel medic plantlets cultured in vitro, challenged with distinct stress agents (copper and PEG, respectively). A parallel investigation was carried out on the *top1* genes and this choice was determined by the fact that, in animal cells, the so far best-characterized role played by Tdp1 is related to the repair of topo I-mediated DNA damage (Yang et al. 1996). Since in animals both functions are tightly linked to each other and to the stress response, this specific relationship was thus explored, for the first time, also in planta, utilizing treatments with two distinct stress agents, copper and PEG.

It is known that exposure of plants to high doses of redox active heavy metals such as copper leads to ROS accumulation and to oxidative damage (Schutzendubel and Polle 2002). Copper-responsive genes coding for signal transduction components have been investigated in *Medicago sativa* by Jonak et al. (2004). Treatments with PEG have been used to study the plant response to osmotic stress and more recently to explore the molecular and cellular mechanisms involved in the plant antioxidant response (Wang et al. 2005).

The effects of oxidative stress on barrel medic plantlets were first analyzed in terms of growth rates, chlorophyll content and free proline accumulation. Both the stress agents negatively affected plant growth, causing a significant reduction in the average fresh weight of aerial parts

and roots. It is worth noting that the chlorophyll content significantly increased in the aerial parts of barrel medic plantlets in which copper was accumulated and this might result from a compensatory mechanism for copper-mediated stress, since it has been documented that toxic doses of the metal interfere with the biosynthesis of the photosynthetic machinery (Prasad et al. 2001). An increase in chlorophyll content was also detected in response to PEG 6000 treatment, in accordance with the recent observation that *M. truncatula*, a plant well adapted to semi-arid conditions, possesses a leaf photochemistry resistant to water shortage (Nunes et al. 2008). The response to copper and PEG treatments in barrel medic was accompanied by significant accumulation of free proline. It is interesting to note that several functions have been ascribed to proline in addition to the classic role in osmotic adjustment, such as free radical scavenging and stabilization of intracellular structures (Takagi 2008). Results from the present investigation are in agreement with the study carried out by Armengaud et al. (2004) who reported the accumulation of free proline in response to hyperosmotic stress in *M. truncatula*.

Accumulation of hydrogen peroxide and superoxide radicals in the aerial parts of barrel medic plantlets is consistent with the uptake of high copper doses, responsible for ROS production caused by autoxidation and Fenton reactions (Schutzendubel and Polle 2002). The increased ROS production in PEG-treated barrel medic leaf tissues is in agreement with data reported in previous studies demonstrating that hydrogen peroxide is accumulated when PEG treatments are imposed (Gengsheng et al. 2000).

Due to the relevant role played by the animal Tdp1 and topo I enzymes in DNA repair, the effects of stress treatments were also evaluated in terms of oxidative DNA damage, an aspect still poorly explored in plants. The significantly increased ROS production in leaf tissues of treated barrel medic plantlets was consistent with the level of oxidative DNA damage measured in terms of 8-oxo-dG (the most common purine base redox lesion formed in vivo in animal cells), which is mainly removed by the BER pathway (Dizdaroglu 2005). The reported values are similar to those obtained in other plant species, such as *Daucus carota* (Balestrazzi et al. 2010) and *Populus alba* (Balestrazzi et al. 2009), in which oxidative DNA damage induced by UV-C radiation and copper, respectively, was also evaluated using an ELISA assay.

The main goal of the present work was to acquire information on the expression profiles of *MtTdp1* genes. QRT-PCR experiments clearly demonstrated that the *MtTdp1* genes are responsive to toxic copper doses. The *MtTdp1* genes were also significantly up-regulated in aerial parts and roots of plantlets exposed to PEG 6000 treatment. The finding that both *MtTdp1* genes were responsive to distinct agents imposed during independent tests suggests a require-

ment of the Tdp1 function under stress conditions. From this point of view, the response of *MtTdp1* genes to stress seems to be in agreement with the literature available on the animal *Tdp1* gene (Lu et al. 2004).

With regard to the response of *top1* genes, only the *top1β* gene was up-regulated in barrel medic plantlets treated with increasing copper and PEG 6000 concentrations. It is worth noting that regarding the possible role played in planta by the α and β topo I isoforms, Takahashi et al. (2002) presented two distinct hypotheses. Since it has been reported that the N-terminal region of topo I mediates the interaction of the enzyme with other proteins, the finding that the α and β isoforms possess poorly conserved N-terminal domains suggests their possible interaction with different proteins. This observation supports the different roles in planta for each topo I isoform. The second hypothesis is based on the existence of a functional equivalence of the two isoforms. The reported data, describing the expression profiles of the *top1* genes in barrel medic, demonstrate that only the *top1β* gene is involved in the plant antioxidant response, possibly indicating the existence of different roles. On the other hand, the topo Iβ isoform has been previously described as the "classical" isoform, due to its homology with the enzyme identified in higher eukaryotes, while the role of the α isoform is still controversial (Balestrazzi et al. 2000, 2010).

It is generally acknowledged that genes involved in DNA and RNA metabolism are regulated not only with respect to physiological processes, but also in response to environmental stresses. This is the case of the pea (*Pisum sativum*) DNA helicase 45, which has been expressed in tobacco, providing high salinity tolerance without affecting productivity (Sanan-Mishra et al. 2005) while it has been reported that the pea *top2* gene, encoding DNA topoisomerase II, has a stress-responsive promoter (Hettiarachchi et al. 2005). More recently, Luo et al. (2009) demonstrated that the expression of a putative helicase gene from *Medicago sativa* in *A. thaliana* enhanced the activity of ROS scavenging enzymes, as well as proline content, under salt and drought stress.

The *APX* gene encoding cytosolic ascorbate peroxidase was chosen as molecular marker of the antioxidant response outside the nucleus. Among the isozymes of ascorbate peroxidase, the cytosolic isoform is highly responsive to several environmental changes, while the corresponding genes are up-regulated by H_2O_2 accumulation (Ishikawa and Shigeoka 2008). The observed expression profiles of the *APX* gene confirmed that the antioxidant mechanisms were activated in the aerial parts of barrel medic plantlets challenged with copper and PEG 6000, while the lack of significant changes in *APX* mRNA levels evidenced in roots might suggest the occurrence of post-translational regulation of APX. On the other hand, it is

known that the levels of cytosolic APX protein and transcript not always correlate and that each APX isoenzyme is individually regulated within a specific cellular compartment in response to stress to minimize oxidative damage (Yoshimura et al. 2000).

Since no data are currently available concerning the ROS amounts and the possible level of oxidative DNA damage in barrel medic roots, the observed response of *Tdp1* genes in these tissues within the plant antioxidant context still needs confirmation. Furthermore, considering the extended time period of both copper and PEG 6000 treatments, we cannot exclude the possibility that the prolonged exposure of barrel medic plantlets to these stress agents might have activated some adaptation responses. Up-regulation of genes involved in secondary metabolism and biosynthesis of antioxidants has been described as an integral part of adaptation to water stress in lettuce (*Lactuca sativa*) (Oh et al. 2008). Similarly, accumulation of soluble sugars and free amino acids, such as proline, in different plant organs, can induce an adaptive response to copper (El-Tayeb et al. 2006). Furthermore, the differential roles of metal-binding proteins in the metal-adaptive response have been recently highlighted in plants (Murali Achary and Panda 2009). Besides these considerations, it should be also underlined that up-regulation of both *MtTdp1* and *top1* genes occurred during seed imbibition, a physiological event requiring DNA repair.

Due to the relevant role played by the animal *Tdp1* gene in DNA repair, the expression patterns of the *MtTdp1* genes were investigated during seed imbibition, a process requiring active DNA repair. It is known that water uptake during seed rehydration leads to resumption of respiratory activity and protein synthesis, followed by several cellular and biochemical events, among which DNA repair plays an essential role to guarantee genome stability. An extension of the G1 phase, occurring during seed imbibition, allows pre-replicative DNA repair, thus preventing the possible deleterious effects derived from a damaged template (Whittle et al. 2001). Although both the *MtTdp1* genes were significantly up-regulated during seed rehydration, a temporal shift in transcript accumulation was observed, since the *MtTdp1α* and *β* mRNAs peaked at 12 and 8 h, respectively. The reported data also highlight the demand for both transcripts during this critical step of seed germination.

In animal cells multiple roles have been so far ascribed to topo I, not only acting as a sensor of DNA damage, but also playing an effector role in DNA repair processes (Lebedeva et al. 2008); no information concerning this topic is currently available in plants. Interestingly, the occurrence of two distinct *top1* genes poses the question on the specific contribution of each topo I isoform to DNA repair. The expression levels of *top1α* and *top1β* genes in seeds at 8 h of rehydration suggest the predominant require-

ment of the topo Iα isoform, at least in seeds, in plant DNA repair, differently from that observed in response to copper and PEG treatments. The subsequent increase in the *top1α* mRNA level occurring at 36 h might be explained considering the increased transcriptional rates, which accompany resumption of DNA synthesis and cell division, as reported in the case of tomato (*Lycopersicon esculentum*) embryos (de Castro et al. 2000).

Further investigation on the *top1* genes will help in understanding the biological relevance of the repair pathways, which involve the topo I enzyme (Lebedeva et al. 2008). In animal cells, topo I is involved in the NER pathway, as demonstrated by Mielke et al. (2007). The finding that mitomycin C, which causes DNA double-strand breaks repaired by NER, can induce a consistent increase of cell death rate in carrot topo I-depleted cells (Balestrazzi et al. 2010) further supports the hypothesis of an active role of these enzymes in DNA repair processes, also in plants.

To date, information on the expression patterns of specific DNA repair genes in plants is still scanty. Lima et al. (2001) analyzed the DNA repair-related ESTs in sugarcane and demonstrated that genes involved in the NER pathway were less expressed in seeds compared to other tissues. Furthermore, expression of those genes participating in the BER pathway was not detected in seeds. This finding might suggest that sugarcane seeds have the DNA repair enzymes stored in the embryo. In contrast, reported data from barrel medic seem to suggest the requirement of newly synthesized *Tdp1* and *top1* mRNAs during seed rehydration, concomitant with the resumption of DNA repair.

Although additional experimental work will be required to better explain the putative roles played by the MtTdp1 isoforms, taking advantage of more straightforward approaches, such as protein-based analyses, the reported data strongly support the use of the *MtTdp1* cDNAs for in planta over-expression studies, aimed at the production of novel stress-tolerant genotypes.

Another relevant part of information obtained with the present study is related to the quantitation of oxidative DNA damage in barrel medic seeds. Considerable evidence exists that ROS are involved in different aspects of seed physiology, both as cytotoxic agents and signaling components (Bailly 2004). However, to our knowledge, no reports describing the extent of DNA oxidative lesions in seeds are currently available. The observed accumulation of 8-oxo-dG might be a consequence of ROS production, which takes place during the early phase of seed imbibition.

In conclusion, the present work reports for the first time on the *Tdp1* genes in plants, highlighting the occurrence of a *Tdp1* gene family indicative of different roles played in DNA repair, while results on the *top1* genes expand the current knowledge on their possible in planta roles. Besides this, the use of seed imbibition as a working system to

explore the response of novel genes in DNA repair turned out to be an effective tool, which requires reduced temporal and technical efforts.

References

Armengaud P, Thiery L, Buhot N, Grenier-de March G, Savourè A (2004) Transcriptional regulation of proline biosynthesis in *Medicago truncatula* reveals developmental and environmental specific features. Physiol Plant 120:442–450

Bailly C (2004) Active oxygen species and antioxidants in seed biology. Seed Sci Res 14:93–107

Balestrazzi A, Chini A, Bernacchia G, Bracci A, Luccarini G, Cella R, Carbonera D (2000) Carrot cells contain two *top1* genes having the coding capacity for two distinct DNA topoisomerase I. J Exp Bot 51:1979–1990

Balestrazzi A, Botti S, Zelasco S, Biondi S, Franchin C, Calligari P, Racchi M, Turchi A, Lingua G, Berta G, Carbonera D (2009) Expression of the *PsMT$_{A1}$* gene in white poplar engineered with the MAT system is associated to heavy metal tolerance and protection against 8-hydroxy-2′-deoxyguanosine mediated-DNA damage. Plant Cell Rep 28:1179–1192

Balestrazzi A, Locato V, Bottone MG, De Gara L, Biggiogera M, Pellicciari C, Botti S, Di Gesù D, Donà M, Carbonera D (2010) Response to UV-C radiation in topo I-deficient carrot cells with low ascorbate levels. J Exp Bot 61:575–585

Bates LS, Waldren RP, Teare ID (1973) Rapid determination of free proline for water-stress studies. Plant Soil 270:343–353

Brameier M, Krings A, MacCallum RM (2007) NucPred-predicting nuclear localization of proteins. Bioinformatics 23:1159–1160

Brunner AM, Jakovlev IA, Strauss SH (2004) Validating internal controls for quantitative plant gene expression studies. BMC Plant Biol 4:14

Bustin SA (2000) Absolute quantification of mRNA using real-time reverse transcription polymerase chain reaction assays. J Mol Endocrinol 25:169–193

de Castro RD, van Lammeren AAM, Groot SPC, Bino RJ, Hilhorst HWM (2000) Cell division and subsequent radicle protrusion in tomato seeds are inhibited by osmotic stress but DNA synthesis and formation of microtubular cytoskeleton are not. Plant Physiol 122:327–335

El-Khamisy SF, Saifi GM, Weinfeld M, Johansson F, Helleday T, Lupski JR, Caldecott KW (2005) Defective DNA single-strand break repair in spinocerebellar ataxia with axonal neuropathy. Nature 434:108–113

El-Tayeb MA, El-Enany AE, Ahmed NL (2006) Salycilic acid-induced adaptive response to copper stress in sunflower (*Helianthus annuus* L.). Plant Growth Regul 50:191–199

Fryer MJ, Oxborough K, Mullineaux PM, Baker NR (2002) Imaging of photooxidative stress responses in leaves. J Exp Bot 53:1249–1254

Gengsh.ong X, Kairong C, Ji L, Yafu W, Zhixiao L (2000) Water stress and accumulation of β-N-oxalyl-L-α, β-diaminopropionic acid in grass pea (*Lathyrus sativus*). J Agric Food Chem 49:216–220

Hettiarachchi GH, Reddy MK, Sopory SK, Chattopadhyay S (2005) Regulation of TOP2 by various abiotic stresses including cold and salinity in pea and transgenic tobacco plants. Plant Cell Physiol 46:1154–1160

Inamdar KV, Pouliot JJ, Zhou T, Lees-Miller SP, Rasouli-Nia A, Povirk LF (2002) Conversion of phosphoglycolate to phosphate termini on 3′-overhangs of DNA double strand breaks by the human tyrosyl-DNA phosphodiesterase hTdp1. J Biol Chem 277:27162–27168

Interthal H, Pouliot JJ, Champoux JJ (2001) The tyrosyl-DNA phosphodiesterase Tdp1 is a member of the phospholipase D superfamily. Proc Natl Acad Sci USA 98:12009–12014

Ishikawa T, Shigeoka S (2008) Recent advances in ascorbate biosynthesis and the physiological significance of ascorbate peroxidase in photosynthesizing organisms. Biosci Biotech Biochem 72:1143–1154

Jonak C, Nakagami H, Hirt H (2004) Heavy metal stress. Activation of distinct mitogen-activated protein kinase pathways by copper and cadmium. Plant Physiol 136:3276–3283

Kimura S, Sakaguchi K (2006) DNA repair in plants. Chem Rev 106:753–766

Lebedeva N, Rechkunova N, Boiteux S, Lavrik O (2008) Trapping of human DNA topoisomerase I by DNA structures mimicking intermediates of DNA repair. IUBMB Life 60:130–134

Lima WC, Medina-Silva R, Galhardo RS, Menck CFM (2001) Distribution of DNA repair-related ESTs in sugarcane. Gen Mol Biol 24:141–146

Locato V, Balestrazzi A, De Gara L, Carbonera D (2006) Reduced expression of *top1β* gene induces programmed cell death and alters ascorbate metabolism in *Daucus carota* cultured cell. J Exp Bot 57:1667–1676

Lu T, Pan Y, Kao SY, Li C, Kohane I, Chan J, Yankner BA (2004) Gene regulation and DNA damage in the ageing human brain. Nature 429:883–891

Luo Y, Liu YB, Dong YX, Gao X-Q, Zhang XS (2009) Expression of a putative alfalfa helicase increases tolerance to abiotic stress in *Arabidopsis* by enhancing the capacities for ROS scavenging and osmotic adjustments. J Plant Physiol 166:385–394

Mielke C, Kalfalah FM, Christensen MO, Boege F (2007) Rapid and prolonged stalling of human DNA topoisomerase I in UVA-irradiated genomic areas. DNA Repair 6:1757–1763

Miura K, Jin JB, Hasegawa PM (2007) Sumoylation, a post translational regulatory process in plants. Curr Opin Plant Biol 10:495–502

Murali Achary VM, Panda BB (2009) Aluminium-induced DNA damage and adaptive response to genotoxic stress in plant cells are mediated through reactive oxygen intermediates. Mutagenesis 25:201–209

Murashige T, Skoog F (1962) A revised medium for rapid growth and bioassays with tobacco tissue culture. Physiol Plant 15:73–79

Nunes C, de Sousa-Araujo S, Marques da Silva J, Fevereiro MPS, Bernardes da Silva A (2008) Physiological responses of the legume model *Medicago truncatula* cv Jemalong to water deficit. Environ Exp Bot 63:289–296

Oh M-N, Trick HN, Rajashekar CB (2008) Secondary metabolism and antioxidants are involved in environmental adaptation and stress tolerance in lettuce. J Plant Physiol 166:180–191

Pommier Y, Redon C, Rao VA, Seiler JA, Sordet O, Takemura H, Antony S, Meng L, Liao Z, Kohlhagen G, Zhang H, Kohn KW (2003) Repair of and checkpoint response to topoisomerase I-mediated DNA damage. Mutat Res 532:173–203

Prasad MNV, Malec P, Waloszek A (2001) Physical responses of *Lemna trisulca* L. to cadmium and copper bioaccumulation. Plant Sci 161:881–889

Ramakers C, Ruijter JM, Lekanne Deprez RH, Moorman AFM (2003) Assumption-free analysis of quantitative real-time polymerase chain reaction (PCR) data. Neurosci Lett 339:62–66

Rogers SO, Bendich AJ (1989) Extraction of DNA from plant tissues. In: Gelvin SB, Schilperoort RA (eds) Plant molecular biology manual. Kluwer Academic Publishers, Dordrecht, pp 1–10

Sambrook J, Fritsch EF, Maniatis T (1989) Molecular cloning: a laboratory manual. Cold Spring Harbor Laboratory Press, Cold Spring Harbor

Sanan-Mishra N, Pham XH, Sopory SK, Tuteja N (2005) Pea DNA helicase 45 overexpression in tobacco confers high salinity tolerance without affecting yield. Proc Natl Acad Sci USA 102:509–514

Schenk RV, Hildebrandt AC (1972) Medium and techniques for induction and growth of monocotyledonous and dicotyledonous plant cell cultures. Can J Bot 50:199–204

Schoeffler AJ, Berger JM (2008) DNA topoisomerases: harnessing and constraining energy to govern chromosome topology. Q Rev Biophys 41:41–101

Schutzendubel A, Polle A (2002) Plant responses to abiotic stresses: heavy metal-induced oxidative stress and protection by mycorrhization. J Exp Bot 53:1351–1365

Singh BN, Sopory SK, Reddy MK (2004) Plant DNA topoisomerases: structure, function and cellular roles in plant development. Crit Rev Plant Sci 23:251–269

Takagi H (2008) Proline as a stress protectant in yeast: physiological functions, metabolic regulations, and biotechnological applications. Appl Microb Biotech 81:211–223

Takahashi T, Matsuhara S, Abe M, Komeda Y (2002) Disruption of a DNA topoisomerase I gene affects morphogenesis in Arabidopsis. Plant Cell 14:2085–2093

Takashima H, Boerkoel CF, John J, Saifi GM, Salih MA, Armostrong D, Mao Y, Quiocho FA, Roa BB, Nakagawa M, Stockton DW, Lupski JR (2002) Mutation of TDP1, encoding a topoisomerase I-dependent DNA damage repair enzyme, in spinocerebellar ataxia with axonal neuropathy. Nat Genet 32:267–272

Thordal-Christensen H, Zhang Z, Wei Y, Collinge DB (1997) Subcellular localization of H_2O_2 in plants. H_2O_2 accumulation in papillae and hypersensitive response during the barley—powdery mildew interaction. Plant J 11:1187–1194

Trinh TH, Ratet P, Kondorosi E, Durand P, Kamatè K, Bauer P, Kondorosi A (1998) Rapid and efficient transformation of diploid *Medicago truncatula* and *Medicago sativa* ssp. falcata lines improved in somatic embryogenesis. Plant Cell Rep 17:345–355

Wang F-Z, Wang Q-B, Kwon S-Y, Kwak S-S, Su W-A (2005) Enhanced drought tolerance of transgenic rice plants expressing a pea manganese superoxide dismutase. J Plant Physiol 162:465–472

Wellburn AR (1994) The spectral determination of chlorophylls *a* and *b*, as well as total carotenoids, using various solvents with spectrophotometers of different resolution. J Plant Physiol 144:307–313

Whittle C-A, Beardmore T, Johnston MO (2001) Is G1 arrest in plant seeds induced by a p53-related pathway? Trends Plant Sci 6:248–251

Yang SW, Burgin AB Jr, Huizenga BN, Robertson CA, Yao KC, Nash HA (1996) A eukaryotic enzyme that can disjoin dead-end covalent complexes between DNA and type I topoisomerases. Proc Natl Acad Sci USA 93:11534–11539

Yoshimura K, Yabuta Y, Ishikawa T, Shigeoka S (2000) Expression of spinach ascorbate peroxidase isoenzymes in response to oxidative stress. Plant Physiol 123:223–233

Yurchenko V, Xue Z, Sadofsky MJ (2006) SUMO modification of human XRCC4 regulates its localization and function in DNA double-strand break repair. Mol Cell Biol 26:1786–1794